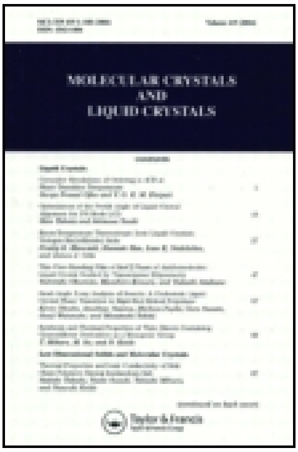

Molecular Crystals and Liquid Crystals
Publication details, including instructions for authors and subscription information:
http://www.tandfonline.com/loi/gmcl20

Anomalous Deformation of Smectic Bubbles under DC Electric Field

Yoko Ishii [a], Shin-Ya Sugisawa [a] & Yuka Tabe [a]

[a] Department of Physics and Applied Physics, Waseda University, 3-4-1 Okubo, 169-8555 Tokyo, Japan

Version of record first published: 07 Oct 2011

To cite this article: Yoko Ishii, Shin-Ya Sugisawa & Yuka Tabe (2011): Anomalous Deformation of Smectic Bubbles under DC Electric Field, Molecular Crystals and Liquid Crystals, 549:1, 166-173

To link to this article: http://dx.doi.org/10.1080/15421406.2011.581151

Mol. Cryst. Liq. Cryst., Vol. 549: pp. 166–173, 2011

ISSN: 1542-1406 print/1563-5287 online
DOI: 10.1080/15421406.2011.581151

Anomalous Deformation of Smectic Bubbles under DC Electric Field

YOKO ISHII, SHIN-YA SUGISAWA, AND YUKA TABE*

Department of Physics and Applied Physics, Waseda University, 3-4-1 Okubo, 169-8555 Tokyo, Japan

Hemispherical bubbles composed of smectic liquid crystals show an unusual deformation under DC electric field. When the lower voltage than a threshold is applied to the bubble on a substrate, it is elongated in the direction of the electric field and forms a semi-elliptical shape in the equilibrium. With the higher voltage than the threshold, the bubble becomes unstable and sometimes exhibits a periodic oscillation with repeating the elongation and shrinkage. Based on a simple equation of force balance, we analyzed both the static and dynamic deformations under DC field and successfully reproduced the observed behaviour. By the detailed analysis, we also determined the surface tension and the electric conductivity of the smectic bubbles.

1. Introduction

Thin films composed of softly condensed matter such as biomembranes, soap bubbles and polymer films have been studied for long years from the points of view of both basic science and application. A common feature of these films is the coexistence of the robustness and the flexibility, which plays an essential role in their functions and sometimes enables them to cause surprisingly large transformations [1]. Since the deformations reflect the intrinsic character of the samples, it is possible to determine some physical properties by quantitatively analyzing them. For instance, when a film is deformed under a certain external field and reaches an equilibrium shape, the external force should be balanced with the internal restoring force. If the deformation is large enough to be measured, from the result, we can estimate the value of the physical property responsible to the external field and also the internal restoring force. In order to visualize the immanent properties through the deformations, it is convenient to use bubbles (vesicles in solutions) than flat films because they can more freely change the shapes.

Based on this idea, we previously studied the deformations of soft bubbles composed of smectic liquid crystals (LCs) under chemical potential gradients, and by the detailed analysis of the deformations, quantitatively determined the gaseous permeability of the LC films [2]. Compared to soap bubbles, the smectic bubbles have the advantage of robustness and sustainability, and the information about their physical properties will be useful for LC device industry.

In this paper, we examine the deformations of smectic bubbles under DC electric field. Since the field is DC, the force acting the bubbles is the electrostatic force, which pulls the bubbles against the surface tension. Generally, if there are two competitive forces

*Corresponding author. E-mail: tabe@waseda.jp

in one system, the equilibrium state is realized when the forces are balanced with each other. But if the response time of the system to two forces are considerably different, the static equilibrium cannot be reached but instead time-dependent non-equilibrium dynamics sometimes appear [3,4]. Since the smectic bubbles under DC electric field are subjected to the competing electrostatic force and surface tension, both the static deformation and the dynamic oscillation are observed in the experiment, the type of which depends on the magnitude of the applied field. We will analyze both the deformations by a simple model.

2. Experimental

The LC compound we used in the experiment was 4-n-octyl-4′-cyanobiphenyl (8CB; Cr 21.5 SmA 33.5 N 40.5 I), which takes stable smectic-A phase around the room temperature. The hemispherical bubbles were first made with a capillary and set on a stainless plate with 15 mm diameter. The initial radii and the thicknesses of the bubbles were 1–3 mm and 200–600 nm, respectively, where the film thickness was determined by the reflectivity measurement[5]. In order to apply DC electric field, the stainless plate supporting the bubble was used as one side of the electrodes, and as the upper electrodes, we prepared two types, one of which was the same flat substrate as the bottom and the other had a cone-like shape. DC power supply generates 0∼2500 DC volts, and the distance between the two electrodes can be varied by a controllable z-stage. The shapes of the bubbles were observed by high-speed camera Photron APX-RS. All the experiments were done at room temperature.

3. Results and Discussion

At first, we used the flat stainless plate as the upper electrode. When a low DC voltage was applied to a hemispherical bubble on the stainless plate, the bubble was elongated in the direction of the electric field (z-direction), and as the voltage increased gradually, the deformation (elongation) also became larger as shown in Fig. 1, in which the shape of the bubble is nearly semi-ellipsoidal. With further increase of the voltage to exceed a certain threshold, the speed of the deformation was suddenly accelerated and the top of the bubble touched the upper electrode. About 90% of the bubbles were broken by the collision, but 10% survived and started a periodic oscillation with repeatedly touching and detaching from the electrode.

Let us describe the detailed result of the static and dynamic deformations separately below.

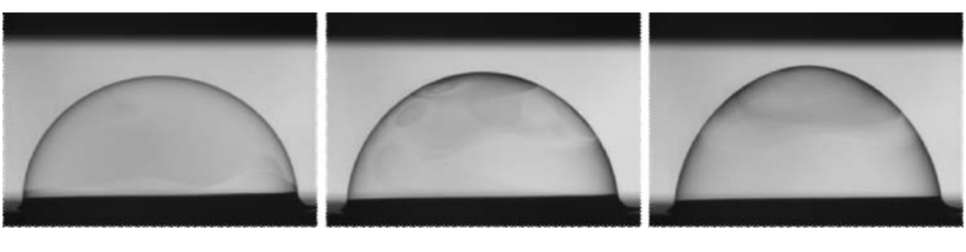

Figure 1. Deformation of hemispherical bubble under DC electric field of (a) 0V, (b) 1000V and (c) 1250V. The initial bubble radius is $r_0 = 2.22$ mm and the electrode distance is $d = 3$ mm.

Static Deformation Under the Lower Electric Field than the Threshold

As is shown in Fig. 1, the bubble is elongated by the DC field and the elongation is increased with the applied voltage. For the quantitative analysis, we define the deformation ratio x as

$$x = \frac{h}{r_0} - 1, \tag{1}$$

where h is the bubble height under the given electric field and r_0 is the initial bubble radius. If the applied voltage is lower than a certain threshold, the bubble reaches an equilibrium state in several seconds after the voltage is on. We gradually increased the voltage below the threshold and measured the equilibrated bubble-height by using several tens of bubbles with various radii. When we compared the data of x and the applied electric field, the relation was neither linear nor quadric.

Before showing more experimental results, let us consider what happens to the smectic bubbles under DC field. It is known that liquid crystals, including 8CB, should have low electric conductivity as $\sim 10^{-8}\Omega^{-1}\text{cm}^{-1}$. Therefore, as the response of the liquid crystals to an electric field, we usually consider the dielectric properties only. But in the present case, since the applied voltage was DC and we waited for long enough to obtain the equilibrium state, the bubble should behave as a conductor. Indeed, when the electric field was turned on, we always observed a hydrodynamic motion in the bubble that carries the real charges. In the equilibrium state under the DC field, therefore, what elongates the bubble is the electrostatic force between the charges on the bubble surface and those on the upper electrode. If the bubble is pulled and elongated, the competitive force, the surface tension, tries to bring it back, and when the two forces are balanced, the bubble reaches the equilibrium state. The total force acting on the bubble film per unit area is given by

$$f_r = \left(p_{in} + \frac{1}{2}\rho E_r\right) - \left(p_0 + 2\sigma\left(\frac{1}{R_1} + \frac{1}{R_2}\right)\right), \tag{2}$$

where p_{in} and p_0 are the pressures inside and outside the bubble, respectively, ρ is the charge density on the bubble surface, E_r is the electric field, σ is the surface tension, and R_1 and R_2 are the principal curvature radii of the deformed bubble. The force must be perpendicular to the bubble surface at any point, and the sign of f_r is taken positive when the force acts from the inside toward the outside. Eq. (2) must be satisfied at each point on the bubble surface including the top area. In order to solve the equation in the equilibrium state ($f_r = 0$), we assume that (i) the deformed bubble shape is semi-ellipsoid, (ii) the molecular number of air inside the bubble is constant and (iii)$Er \approx V\big/(d-h)$at the top of the bubble, where d is the electrode distance and V is the applied voltage. Substituting them into eq. (2) and putting $f_r = 0$, we obtain the normalized force balance equation as

$$x\,(x_d - x)^2 = \frac{\varepsilon_0 V^2}{24\sigma r_0}, \tag{3}$$

in which x_d is defined as $x_d = d/r_0 - 1$, corresponding to the normalized position of the upper electrode. In the realistic region of $0 < x < x_d$, eq. (3) possess two real solutions when $\frac{\varepsilon_0 V^2}{24\sigma r_0} < \frac{4x_d^3}{27}$, among which, the smaller one is the solution that corresponds to the present experiment. Based on eq. (3), we analyzed all the data obtained with the various combinations of bubbles and electrode distances. The result is shown in Fig. 2. The transverse axis is the right side of eq. (3) multiplied by σ, and the vertical axis is the left side of eq. (3). The data under the different conditions are all on the single line, which shows

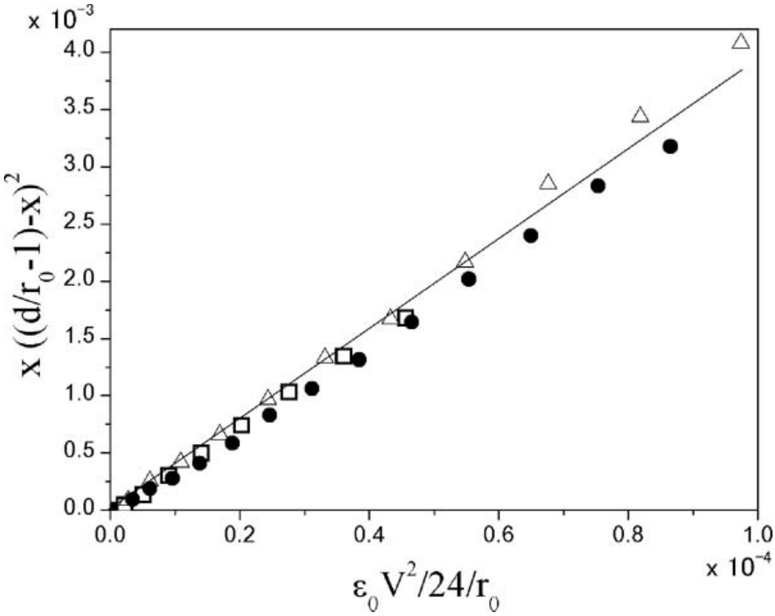

Figure 2. The relation between the normalized deformation ratio and the normalized applied voltage obtained. The open squares, open triangles and filled circles are obtained in the conditions of (r_0, d) = (1.86 mm, 2.4mm), (2.20 mm, 3.0 mm) and (2.74 mm, 3.7 mm), respectively.

the good linear relation with the proportional constant being 40 N/m. Since the slope of the line corresponds to *1/σ*, the surface tension is obtained as $\sigma = 0.025$ N/m. This is close to the previously reported value of σ for 8CB measured by a different method [6].

Next, we focus on the relaxation process of the bubble deformation. Since the force acting on the unit area of the bubble is given by Eq. (2), the equation of motion for the unit area of the bubble top is written as

$$\rho_{LC}\frac{d^2h}{dt^2} + \frac{\nu}{r_0}\frac{dh}{dt} = p_{in} - p_0 - 2\sigma\left(\frac{1}{R_1} + \frac{1}{R_2}\right) + \frac{1}{2}\rho E_r, \tag{4}$$

where ρ_{LC} is the mass density of the smectic bubble per unit of area and ν presents the effective viscosity for the bubble with radius r_0 to move in the air. In this equation, the important point is that E_r depends on the time. Because the smectic bubble is a bad conductor, the time to accumulate the charges on the bubble surface should almost determine the relaxation time of the deformation. In order to calculate the time-dependent electric field, we consider the virtual electric circuit equivalent to the real system as shown in Fig. 3, in which the bubble is replaced by the combination of a capacitor with capacitance C and a resistor with resistance R in series. In the configuration of Fig. 3, the charge stored by the capacitor (the bubble, in the reality) is easily calculated and the electric field of the bubble top is given as

$$E_r \approx \frac{V\left(1 - \exp\left(-\frac{t}{RC}\right)\right)}{d - h}. \tag{5}$$

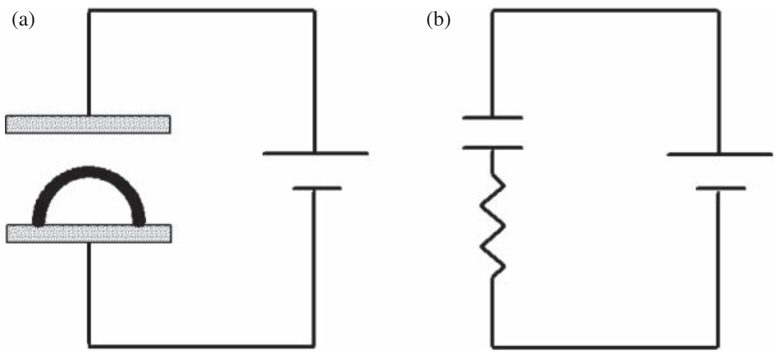

Figure 3. The real situation of (a) is replaced by the RC circuit of (b). The bubble is regarded as the combination of a resister and a capacitor in series.

Substituting Eq. (5) into Eq. (4) and normalizing, we obtain the final form of equation of motion as

$$A\frac{dx(\tau)}{d\tau} = \frac{E(1-e^{-\tau})^2}{(x_d - x(\tau))^2} - x(\tau), \tag{6}$$

with

$$A = \frac{\nu r_0}{12\sigma RC}, \quad E = \frac{\varepsilon_0 V^2}{24\sigma r_0}, \quad \tau = \frac{t}{RC}. \tag{7}$$

Since the inertia term is much smaller than the viscous term, it is neglected in the final form of Eq. (6). Taking the fact into account that the charge accumulation occurs much slower than the bubble deformation in the present regime, we put the left side of Eq. (6) at zero, and obtain the time-dependent bubble deformation equation as

$$x(\tau)(x_d - x(\tau))^2 = E(1-e^{-\tau})^2. \tag{8}$$

We traced the relaxation processes of the bubbles with comparing them to Eq. (8). Figure 4 shows the result when we used two bubbles with the radii of 1.65 mm and 1.85 mm under the applied voltages of 1000 V and 1200 V, respectively. The fitting curves calculated according to Eq. (8) are given by solid lines, both of which follow the experimental result. The data- fitting gives the value of RC, which is found to be about 1 second in both cases. Since the capacitance of the system composed of a flat plate and a sphere with radius r_0 is calculated as $4\pi\varepsilon_0 r_0$, we can estimate the resistance of the bubbles as a few Tera ohm.

Oscillation Under the Higher Electric Field Than the Threshold

Next, we examined the bubble deformation under the high DC field. The force balance equation of eq. (3) indicates that when $\frac{\varepsilon_0 V^2}{24\sigma r_0}$ exceeds $\frac{4}{27}x_d^3$, the real solution is only one, which is larger than x_d. Since x_d is the normalized position of the upper electrode, in the reality, there is no solution satisfying the force-balance equation. As a result, in the condition of $V > \sqrt{\frac{96\sigma r_0}{27\varepsilon_0}x_d^3}$, the bubble should rush toward the upper electrode and collide with it, which agrees with our observation.

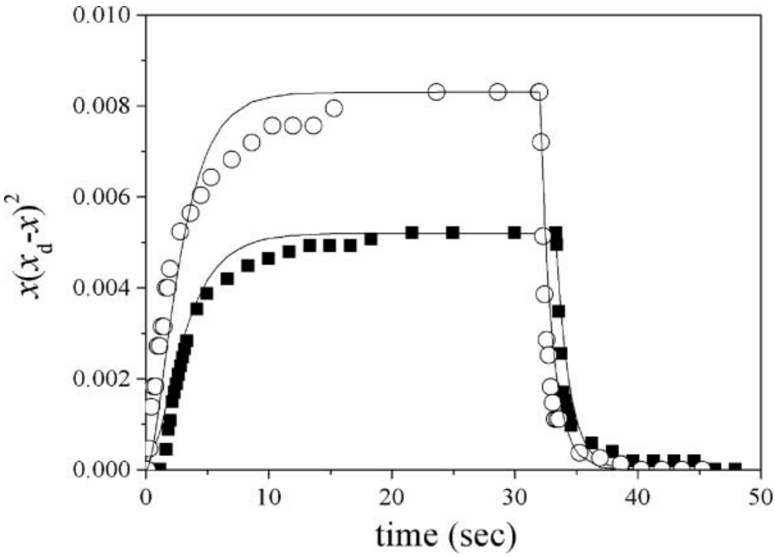

Figure 4. The relaxation of the bubble deformation on and off the applied voltage. The filled squares show the data obtained when the initial bubble radius r_0 is 1.65 mm under the 1000 V and the open circles are for the bubble with $r_0 = 1.85$ mm under 1200 V.

When the bubbles touch the upper electrode, more than 90% were broken, but 10% could survive and then they started a periodic oscillation by repeating the elongation and shrinkage. The typical observation is shown in Fig. 5. In order to stabilize the bubble oscillation, we used the cone-like stainless as the upper electrode in this experiment. The oscillation frequency increases monotonically with the applied voltage, but we could not determine the exact relation between the oscillation frequency and the applied voltage. When the bubble touched the electrode, a small portion of 8CB remained on that, which became a part of the electrode with forming a sharp top. As a result, the shape of the upper electrode was changed by each contact, which changed the electric field at the bubble top. This causes the inconstant frequency of the bubble oscillation even if we use the same-size bubble under the same applied voltage.

Theoretically, the oscillation can be understood as follows: When the applied voltage is switched on, the bubble starts to store the charges. However large the voltage is, in the early stage, the bubble keeps the equilibrium shape to satisfy the force balance given by

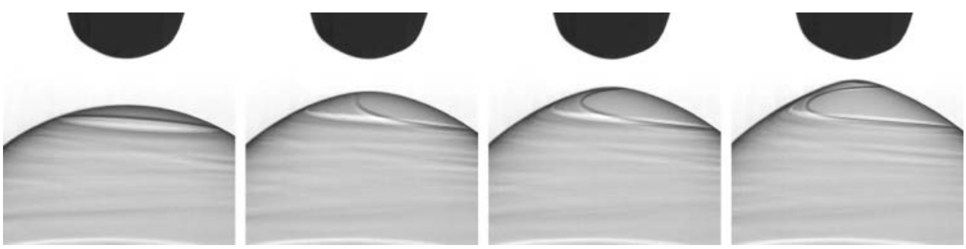

Figure 5. The oscillation of the bubble under 1500VDC. The bubble shape is no more ellipsoid but more like a cone.

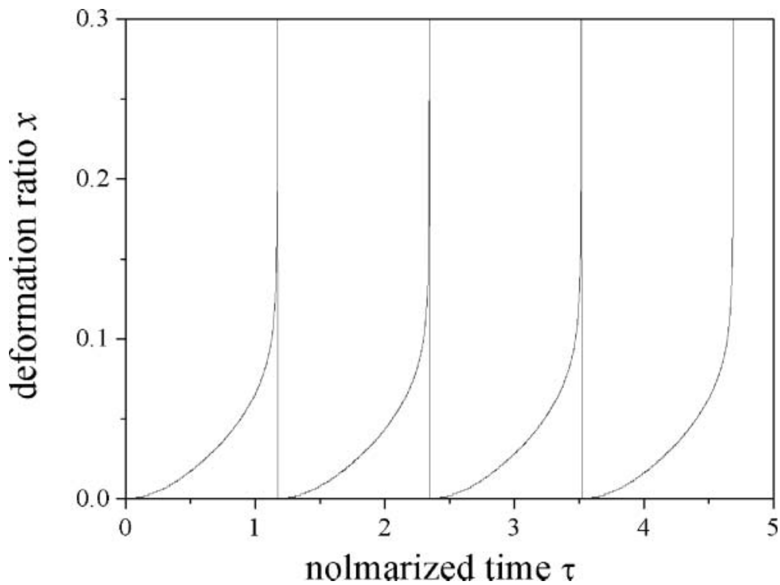

Figure 6. The calculated oscillation of the bubble using Eq. (6).

Eq. (3). If the applied voltage is higher than $\sqrt{\frac{96\sigma r_0}{27\varepsilon_0} x_d^3}$, the charges soon accumulate enough for the electric field to exceed the threshold. Then, the force balance cannot be maintained any more and the bubble rushes toward the upper electrode. At the moment when the bubble touches the electrode, the stored charge on the bubble top moves onto that. Since the electrostatic force is reduced by this charge transfer, the surface tension brings back the bubble into the initial hemi-spherical shape. Then again, the charging will restart, which results in repeating the oscillation.

Based on Eq. (6) and the above analysis, we calculated the dynamic bubble deformation with the conditions given by the experiment. The result is shown in Fig. 6, which qualitatively reproduces the periodic oscillation. However, it was found that the bubble in the experiment did not return to the initial position after the charge transfer but went back to somewhere between $x = 0$ and $x = x_d$, more often near the unstable point of $x = x_d/3$. As the possible reason for the disagreement, we consider that the bubble transfers not all the charges but only a part of them because of the low conductivity. Since the oscillation period strongly depends on the transferred charges, in order to well explain the dynamics, we have to analyze the amount of the charges but so far have not succeeded in the estimation. At this stage, we only show that the DC field-induced bubble dynamics is semi-quantitatively understood by the simple model.

4. Conclusion

We studied static and dynamic deformations of hemispherical smectic bubbles under DC electric field. Although liquid crystals are generally regarded as insulator, DC field induces real charges on the bubble surface and the bubble is subjected to the electrostatic force, which elongates the bubble in the direction of the electric field. When the applied voltage is lower than the threshold value, the bubbles are slightly elongated to form a semi-ellipsoidal shape in the equilibrium state, where the electrostatic force is balanced with the surface tension. Quantitatively analyzing the equilibrated shape, we determined the values of surface tension and conductivity of the smectic bubbles composed of 8CB. When the higher voltage than the threshold is applied to the bubbles, the deformation exceeds the semi-ellipsoid and the bubbles collide with the upper electrode. After the collision, about 10% of the bubbles survive and exhibit the periodic oscillation associated by elongation and shrinkage.

Both the static deformation and the dynamic oscillation are described by a common simple equation that involves the two competitive forces of the electrostatic and the surface tension. Since the similar oscillations have been found in simple liquids [7], the present system and analysis can be used to comprehensively understand the oscillating phenomena induced by electric fields in soft matter. The result may also be useful for making a micro LC jet for the drug delivery system.

Acknowledgments

This work was supported by KAKENHI (Grant-in-Aid for Science Research) on Priority Area "Soft Matter Physics" from the Ministry of Education, Culture, Sports, Science and Technology of Japan.

References

[1] I. Derenyi, F. Julicher and J. Prost, "Formation and interaction of membrane tubes", *Phys. Rev. Lett.*, 2002, **88**, 228101.
[2] Y. Ishii and Y. Tabe, "Gas permeation of LC films observed by smectic bubble expansion", *EPJE*, 2009, **30**, 257–265.
[3] M. Seul and D. Andelman, "Domain shapes and patterns—The phenomenology of modulated phases", *Science*, 1995, **267**, 476–483.
[4] F.T. Arecchi, S. Boccaletti, and P. Ramazza, "Pattern formation and competition in nonlinear optics", *Phys. Rep. Rev. Phys. Lett.*, 1999, **318**, 1–83.
[5] C. Rosenblatt and N.M. Amer, "Optical determination of smectic-A layer spacing in freely suspended thin films", *Appl. Phys. Lett.*, 1980, **36**, 432–434.
[6] R. Stannarius and C. Cramer, "Surface tension measurements in freely suspended bubbles of thermotropic smectic liquid crystals", *Liq. Cryst.*, 1997, **23**, 371–375.
[7] J.-U. Park, *et al.*, "High-resolution electrohydrodynamic jet printing", *Nat. Mat.*, 2007, **6**, 782–789.